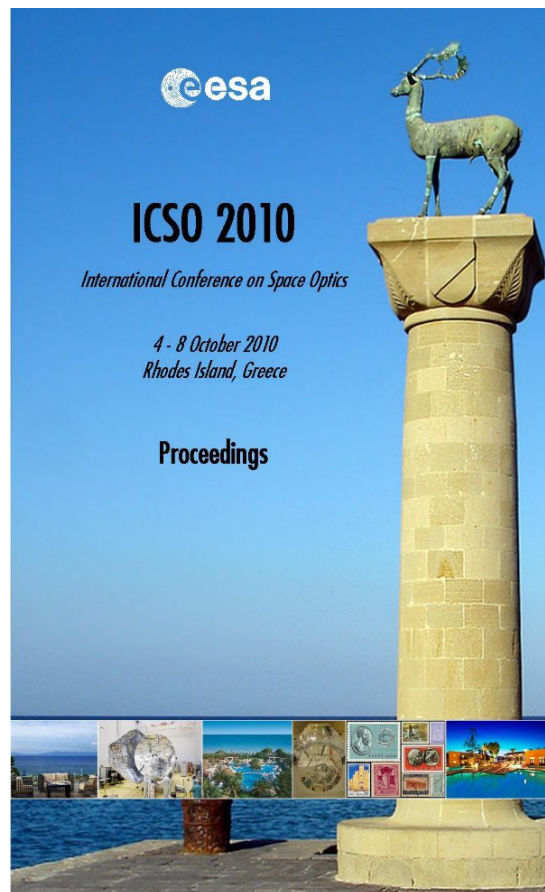


International Conference on Space Optics—ICSO 2010

Rhodes Island, Greece

4–8 October 2010

*Edited by Errico Armandillo, Bruno Cugny,
and Nikos Karafolas*



Spectrograph for solar imaging in the XUV domain

F. Frassetto, S. Coraggia, L. Poletto



International Conference on Space Optics — ICSO 2010, edited by Errico Armandillo, Bruno Cugny,
Nikos Karafolas, Proc. of SPIE Vol. 10565, 105651D · © 2010 ESA and CNES
CCC code: 0277-786X/17/\$18 · doi: 10.1117/12.2309241

SPECTROGRAPH FOR SOLAR IMAGING IN THE XUV DOMAIN

F. Frassetto*, S. Coraggia, L. Poletto

*LUXOR-Institute of Photonics and Nanotechnologies-National Council for Research, via Trasea 7, 35131
Padova, Italy (*frassetto@dei.unipd.it)*

I. ABSTRACT

A new concept for an imaging spectrograph operating at grazing incidence and stigmatic in a large field-of-view is presented. It can acquire both spectral and spatial information at the instrumental focal plane. The design is based on a crossed telescope and on a spherical variable-line-spaced grating. A laboratory prototype working in the spectral range 4–20 nm is presented.

II. INTRODUCTION

Imaging spectrographs for the extreme-ultraviolet (XUV) domain use generally a grating and an entrance slit to separate the spectral from the spatial information. If the spectrograph is stigmatic, a complete map of a two-dimensional region can be obtained by rastering the image in one dimension on the entrance slit. The situation is worse in the case in which the spectrograph is not stigmatic, as most often the case in grazing incidence. In this case the slit must be reduced to a pinhole and the rastering must be performed in two dimensions. The spectroscopic instrument on board SOHO (Solar and Heliospheric Observatory), still working, exemplify the state of the art: the grazing incidence spectrograph configuration (CDS, Coronal Diagnostic Spectrometer) is astigmatic and therefore the scanning of a region on the solar corona needs to be done in two dimensions [1,2].

We present here a new concept for an imaging spectrograph that operates at grazing incidence and is stigmatic in a large field-of-view [3]. The core of the spectrograph is a spherical variable-line-spaced (SVLS) grating giving a focal surface nearly perpendicular to the optical path [4,5]. As a consequence of this, the length of the exit arm of the spectrograph is nearly constant, therefore it is possible to correct for the astigmatism with an auxiliary optics.

The aim of the optical design is to separate the focusing properties in the two spatial directions in order to have two distinct focal points: one in the spectral dispersion plane and the other in the plane parallel to the slit. This is obtained using a double telescope in the Kirkpatrick-Baez configuration [6], and, as a result, the image of an extended source has negligible spectral and spatial broadening in a large field-of-view. Such unique configuration gives monochromatic stigmatic images in an extended field-of-view and in an extended spectral range in the grazing-incidence domain. The spectrograph could be useful for high-resolution spectral imaging of the solar disk in the XUV domain [7]. We have realized a laboratory prototype of such spectrograph working in the 4–20 nm region, with a spectral resolution of 0.1% at 10 nm and a spatial resolution of ≈ 3.5 arcsec over a field-of-view of 0.5° , within a total envelope of 1.3 m. We will present the design and the characterization of the instrument.

III. THE INSTRUMENT

The main instrumental parameters are summarized in Tab. 1. The mechanical structure of the laboratory prototype is sketched in Fig. 1; both the spectral dispersion plane and its perpendicular one are shown. Two pictures of the instrument are presented in Fig. 2.

Tab. 1. Instrumental parameters

Wavelength range	First order: 4 – 20 nm	Spectrometer	Spherical VLS grating
Field-of-view	$\pm 0.25^\circ$	Incidence angle	87°
Telescope 1	Plane Parabolic	Entrance arm	237 mm
Incidence angle	86.5°	Exit arm	235 mm
Size	140 mm \times 30 mm \times 20 mm	Radius	5649 mm
Clear aperture	130 mm \times 10 mm	Size	50 mm \times 30 mm \times 10 mm
Coating	40 nm Ni	Central groove density	1200 gr/mm
Focus to midpoint	600 mm	Parameters for groove space variation	$d_0 = 1200 \text{ mm}^{-1}$ $d_1 = -8.497 \text{ mm}^{-2}$ $d_2 = 5.14 \cdot 10^{-2} \text{ mm}^{-3}$ $d_3 = -3.15 \cdot 10^{-4} \text{ mm}^{-4}$
Telescope 2	Wolter II: plane parabolic + plane hyperbolic	Profile	Saw-tooth, blazed at 10 nm
Incidence angle	Parabolic mirror: 86.5° Hyperbolic mirror: 87.5°	Coating	Gold
Size	Parabolic and Hyperbolic: 140 mm \times 30 mm \times 20 mm	Detector	CCD 16 bit
Clear aperture	Parabolic and Hyperbolic: 130 mm \times 10 mm	Pixel size	20 μm \times 20 μm
Equivalent focal length	1204 mm	Active area	26.8 mm \times 8 mm
Coating	40 nm Ni		

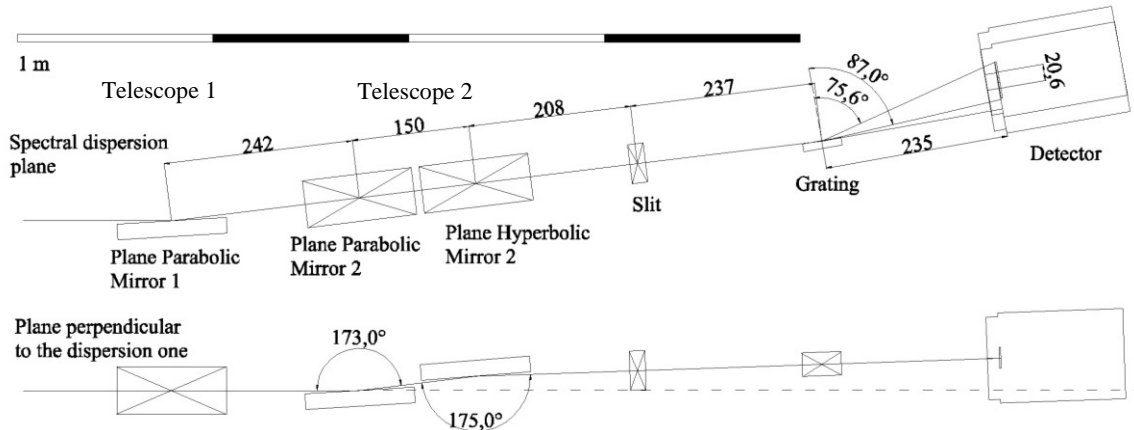


Fig. 1. Optical layout of the instrument. Both the spectral dispersion plane and its perpendicular one are shown. The two focalization directions after the grating are referred to the zero order beam and to the 25 nm radiation. The detector translation necessary to acquire the entire spectral band is 20.6 mm.

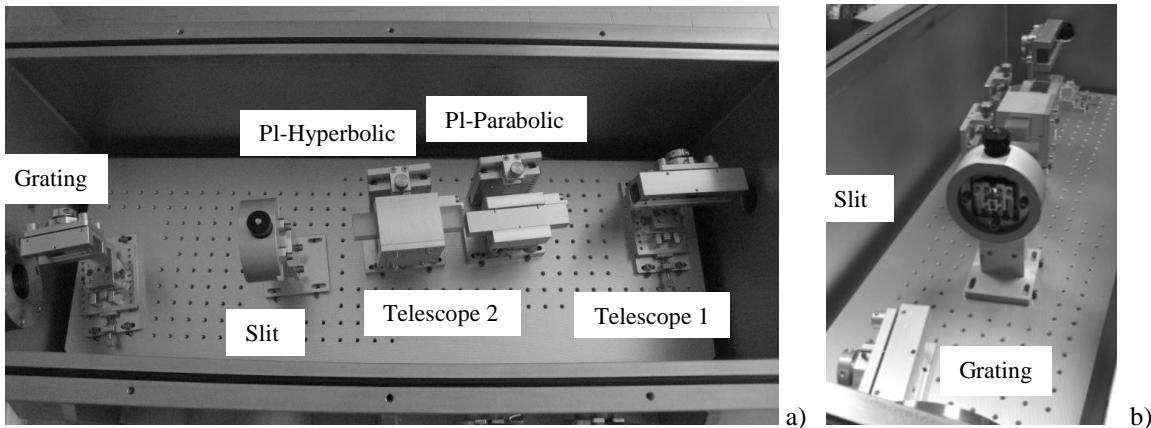


Fig. 2. Images of the laboratory prototype. a) top view, b) detail of the slit – grating section.

A. The Telescope

The imaging capabilities are provided by a crossed telescope in the Kirkpatrick-Baez configuration: the telescope 1 consists of a cylindrical mirror with parabolic section, focusing on the slit of the spectrograph in the spectral dispersion plane; the telescope 2, schematized in Fig. 3, consists of two cylindrical mirrors with aspherical section in Wolter II configuration [8,9], focusing on the focal plane in the direction perpendicular to the spectral dispersion. The telescope 2 is mounted with its tangential plane coincident with the equatorial plane of the telescope 1.

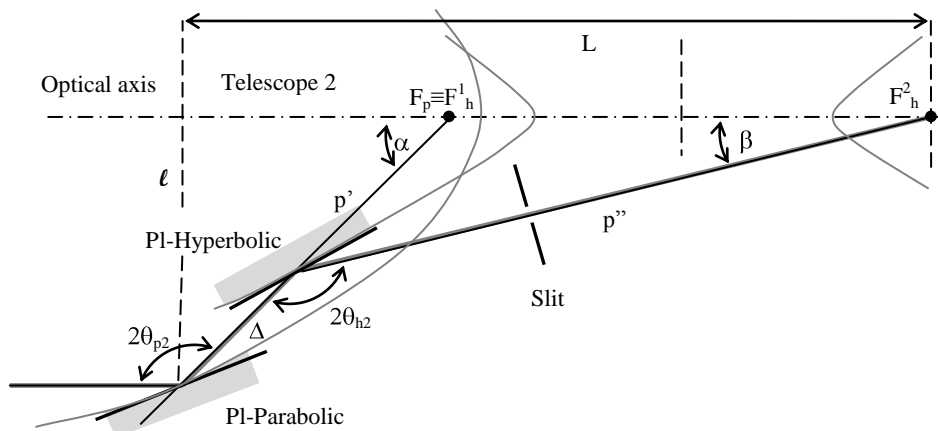


Fig. 3. Detail of the Wolter II telescope. The arrangement of the plane-parabolic/plane-hyperbolic mirrors is shown, and the main geometrical parameters indicated.

The spatial resolution in the direction perpendicular to the slit is given by the telescope 1. The spatial resolution in the direction parallel to the slit, for the off-axis angles also, is instead given by the Wolter II-type telescope 2. The free parameters are: the incidence angle on the parabolic and hyperbolic mirrors θ_{p2} , θ_{h2} , the separation between these two optics Δ , and the exit arm p'' . The connections between these four driving parameters and the other parameters of the telescope are provided by (1-5). In these equations, α and β are the angles formed with the optical axis respectively by the central ray between the two mirrors and by the central ray on the focal plane, p' is the virtual entrance arm of the hyperbolic mirror, f_p and f_h are the focal lengths respectively of the parabolic and hyperbolic mirrors. a and b are the hyperbolic parameters, ℓ is the distance between the center of the first mirror and the optical axis, and L is the distance, measured along the optical axis, from the center of the first mirror to the focal plane.

$$\alpha = \pi - 2\theta_{p2}, \quad \beta = 2\theta_{h2} - 2\theta_{p2} \quad (1)$$

$$p' = p'' \frac{\sin \beta}{\sin \alpha} \quad (2)$$

$$f_p = (p' + \Delta) \cos^2 \theta_{p2}, \quad f_h = \frac{p'' \cos \beta - p' \cos \alpha}{2} \quad (3)$$

$$a = \frac{p'' - p'}{2}, \quad b = \sqrt{f_h^2 - a^2} \quad (4)$$

$$\ell = (p' + \Delta) \sin \alpha, \quad L = p'' \cos \beta + \Delta \cos \alpha \quad (5)$$

The effective focal length of the second telescope, f_{eff} , can be calculated considering an entrance ray forming an angle δ with the optical axis. Due to this inclination, the focal spot is translated by a quantity Δ on the focal plane, and f_{eff} can be calculated as:

$$f_{\text{eff}} = (p' + \Delta) \left[p'' + \Delta - \Delta \frac{\sin(\pi/2 - \theta_{h2})}{\sin(\pi/2 - \theta_{h2} - \delta)} \right] \left/ \left[p' + \Delta - \Delta \frac{\sin(\pi/2 - \theta_{p2})}{\sin(\pi/2 - \theta_{p2} - \delta)} \right] \right. \quad (6)$$

In the case of a small δ , (6) can be simplified in

$$f_{\text{eff}} = (p' + \Delta) \frac{p''}{p'} \quad (7)$$

that in the considered case is about 1204 mm. In Fig. 4 the spots produced by two beams tilted by $\pm 0.25^\circ$ off-axis are compared with the on axis image. The resulting mean focal length calculated as Δ/δ is 1243 mm.

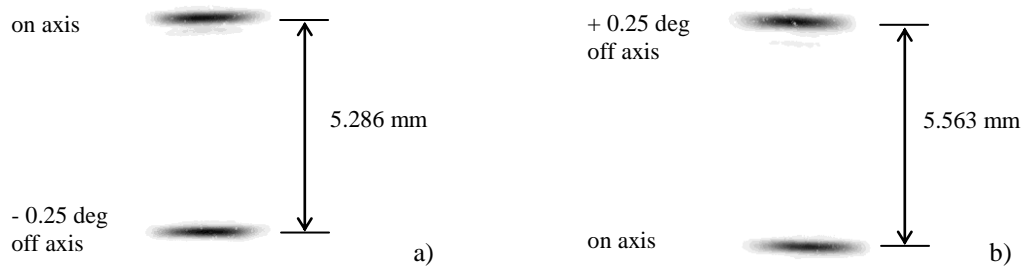


Fig. 4. Spots at the focal plane of the telescope II corresponding to three different conditions: on axis and $\pm 0.25^\circ$ off-axis beam. The spots separation between the on axis and the -0.25° beam, case a), and the on axis and the $+0.25^\circ$ beam, case b), are different due to the not symmetrical telescope arrangement respect to the on axis propagating beam.

B. The Spectrograph

The spectrograph is based on the use of a spherical variable-line-spaced grating. The variation of the groove density is described as

$$d(y) = d_0 + d_1 y + d_2 y^2 + d_3 y^3 \quad (8)$$

where d_0 is the central groove density, d_1 , d_2 and d_3 , the ruling parameters, are optimized to respectively: make the focal curve as close as possible to the detector plane (in the spectral range of interest), minimize the coma, and minimize the spherical aberration.

This optical element has been tested both in our lab and at the BW3 synchrotron beam-line at DORIS storage ring at DESY campus in Hamburg (Germany). The efficiency curve referred to the first diffractive order is

presented in Fig. 5 a): the maximum efficiency is 18%, and is obtained at about 11 nm. In the spectral interval 6 – 30 nm the efficiency is higher than 5%. The contribution of the higher orders, compared to the first one, is shown in Fig. 5. b). An example of acquired spectra at BW3 is presented in Fig. 6, showing the good focalization properties of this element.

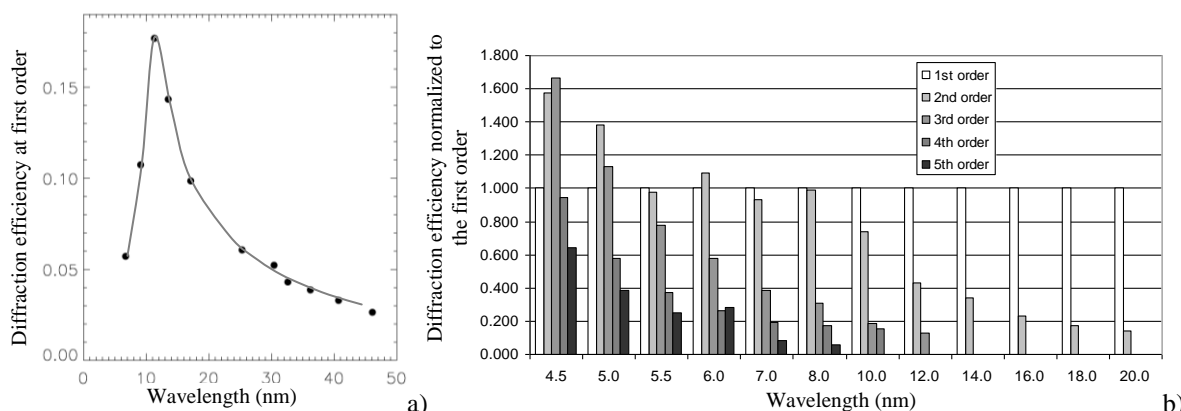


Fig. 5. a) Grating diffraction efficiency at first order. b) Diffraction efficiency at the higher orders compared to the first one.



Fig. 6. Example of a spectra acquired at the BW3 beam-line using the 1200 gr/mm grating, the diffracted wavelength is 3 nm. The multiple orders are clearly visible.

IV. CONCLUSIONS

In this work the innovative concept of an imaging spectrograph working at grazing incidence and stigmatic in a large field-of-view has been presented. The alignment in visible light of a laboratory prototype has been presented. The efficiency performances of the grating, and the focalization properties, have been measured and presented.

REFERENCES

- [1] R.A. Harrison et al., "The Coronal Diagnostic Spectrometer for the Solar and Heliospheric Observatory," *Solar Phys.*, vol. 162, pp. 233-290, 1995
- [2] K.A. Lidiard, P.F. Gray, "Optical Design of the Coronal Diagnostic Spectrometer (an Instrument on the Solar and Heliospheric Observatory)," *Opt. Eng.*, vol. 36, pp. 2311-2319, 1997
- [3] L. Poletto, G. Tondello, "Grazing-incidence telescope-spectrograph for space solar imaging spectroscopy," *Appl. Opt.* vol. 40, pp. 2778-2787, 2001
- [4] T. Kita, T. Harada, N. Nakano, and H. Kuroda, "Mechanically ruled aberration-corrected concave gratings for a flat-field grazing-incidence spectrograph," *Appl. Opt.*, vol. 22, pp. 512-513, 1983
- [5] T. Harada, K. Takahashi, H. Sakuma, A. Osyczka, "Optimum design of a grazing-incidence flat-field spectrograph with a spherical varied-line-space grating," *Appl. Opt.*, vol. 38, pp. 2743-2748, 1999
- [6] P. Kirkpatrick, A.V. Baez, "Formation of optical images by x-rays," *J. Opt. Soc. Am.*, vol. 38, pp. 766-774, 1948
- [7] L. Poletto, G. Tondello, and M. Landini, "EUV and soft x-ray telescope-spectrometer for imaging spectroscopy on the Solar Orbiter mission: grazing-incidence configuration," *Proc. SPIE*, vol. 4498, pp. 39-50, 2001
- [8] H. Wolter, "Mirror systems with glancing incidence as image-producing optics for X-rays," *Ann. Phys.*, vol. 10, pp. 94-114, 1952
- [9] L.P. VanSpeybroeck, R.C. Chase, "Design parameters of paraboloid-hyperboloid telescopes for X-ray astronomy," *Appl. Opt.*, vol. 11, pp. 440-445, 1972